RD42 Internal Note-10
Version: September 27, 1997

Proton Irradiation Study of CVD Diamond Detectors for High Luminosity Experiments at the LHC

PRELIMINARY

The RD42 Collaboration

Abstract

CVD diamond detector samples and one diamond strip detector were irradiated with 24 GeV/c protons at the Proton Synchrotron, PS, in July 1997 at CERN. The detectors received a maximum proton fluence of 5×10^{15} p/cm^2. Detector performance of all diamond samples where characterized before and after irradiation. Particularly charge collection was measured after excitation with electrons from ^{90}Sr at different proton fluences. Charge collection is observed to remain constant up to 1×10^{15} p/cm^2. Charge collection decreases above 2×10^{15} p/cm^2 linearly and reaches 60 % of the unirradiated value at 5×10^{15} p/cm^2. Leakage currents of diamond samples were below 1 pA before irradiation and remain unchanged after irradiation up to the highest fluence. Particle induced currents stay constant at constant proton flux during irradiation.

List of participants

Experimental Realization:
    `DIRK.MEIER@cern.ch`
    `RUDOLF.WEDENIG@cern.ch`
Analysis:
    `DIRK.MEIER@cern.ch`
Authors and Critics received from:
    `KAGAN@mps.ohio-state.edu`
    `DIRK.MEIER@cern.ch`

1 Introduction

CVD diamond detectors were irradiated with protons in order to study their radiation resistance and possible degradation at fluences which are expected in LHC experiments. The proton irradiation of diamonds described in this note is complementary other irradiation studies with gammas, electrons, pions, neutrons and alfas which were studied by RD42 in the past. A first proton irradiation of CVD diamond samples was carried out at TRIUMPF, Canada in 1995 with 500 MeV/c protons up to a final fluence of $\approx \times 10^{14}$ p/cm^2 [1][1]. In June 1997 we irradiated four other CVD diamond samples at the Proton Synchroton, PS, at CERN with a final fluence of 5×10^{15} p/cm^2 and exceeded the TRIUMPF irradiation fluence by at least factor 10. The higher final fluence was possible using a particle flux of more than 10^{10} $p/\mathrm{cm}^2/\mathrm{s}$. The flux attained in the PS irradiation was higher than the flux of 8×10^8 $p/\mathrm{cm}^2/\mathrm{s}$ which was reported for the TRIUMPF irradiation.

1.1 Samples in Proton Irradiation

The irradiated diamond detectors were grown as part of 4" wafers to a thickness of about 700 μm in a chemical vapor deposition (CVD) process [2]. Two samples CDS-12 and CDS-17 (= DBDS-47) with a size of 10×10 mm^2 were used in this proton irradiation. CDS-12 and DBDS-47 were originaly grown to a thickness of 738 μm and 743 μm, respectively. Both samples were processed before irradiation: Sample CDS-12 was lapped on its nucleation (substrate) side by about 20 μm to a final thickness of $\approx$ 715 μm and cut in four equal rectangular pieces CD12-P1,P2,P3 and P4 of 5×5 mm^2. Pieces P1,P2,P3 were taken for irradiation, P4 remained unirradiated as a reference. Sample DBDS-47 was lapped on its substrate side by $\approx$ 300 μm and 50 μm on its growth side to a final thickness of 492 μm. Fig. 1 shows the geometry of the samples CD12-P1,P2,P3 with their electrical contacts, one single dot on their substrate side and a dot with guard ring on their growth side. The contacts are ohmic. Sample DBDS-47 was metalized with a strip tracker mask and a solid electrode on its back.

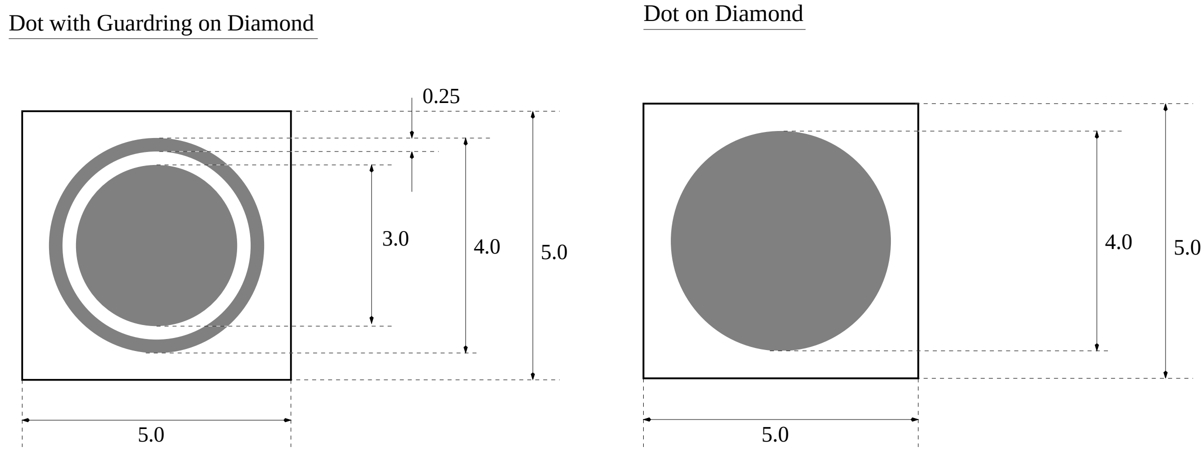

Figure 1: Geometry and size of diamond samples. The diamond samples were metalized with ohmic contacts on both sides. The substrate side had a single round contact, the growth side a round contact and a guard ring.

1.2 Irradiation Setup

A schematic view of the irradiation setup is shown in Fig. 2. The proton beam from the PS is split into different beam lines. The number of protons reaching the experimental areas are

[1] The final fluence of the TRIUMPF irradiation is approximate.

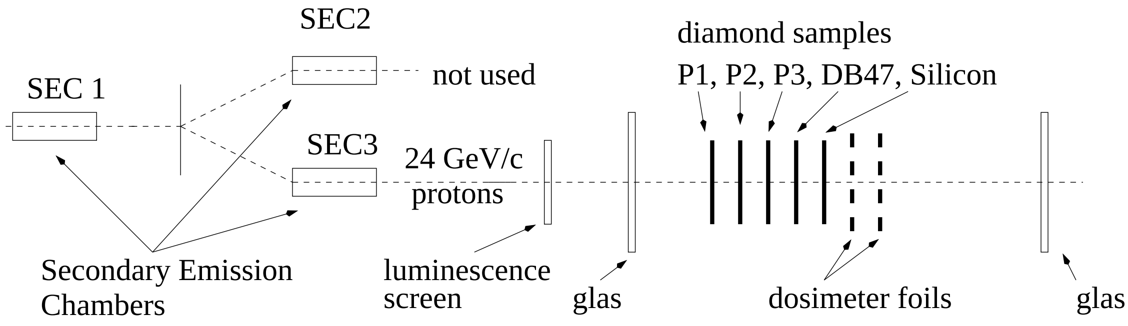

Figure 2: Schematic view of the proton irradiation setup at the PS in zone T7. The proton beam passes two secondary emission chamber SEC1 and SEC3 which measure the proton flux. The beam sweeps over the samples which are adjusted behind each other.

measured by two secondary emission chambers SEC1 and SEC3. These chambers give a charge which is proportional to the number of passing protons. The samples were mounted one after the other in the beam. Their lateral position could be adjusted with a motor. The beam position was verified using two glas plates in front and behind the samples. The glas darkens after $\approx 10^{13}\ p/\mathrm{cm}^2$ and shows the beam spot of highest particle fluence. In order to monitor the presence and actual beam position we used a luminescence screen which was mounted on a motor a few centimeters in front of the irradiation stage. The luminescence light from the proton beam could be observed with a camera as soon as protons swept over screen and samples.

1.3 Dosimetry, Proton Fluence and Flux

The PS delivers protons in spills. Spills can be extracted several times per synchroton cycle. One synchrotron cycle has a length of ≈ 14 s with a spill duration of 300 ms. We were interested to monitor the proton flux using the chamber SEC3. The charge in the secondary emission chamber SEC3 is proportional to the proton flux. Thus we recorded the current signal from SEC3 after each spill. Fig. 3 shows the current from SEC3 as a function of time during the first 60 hours. The

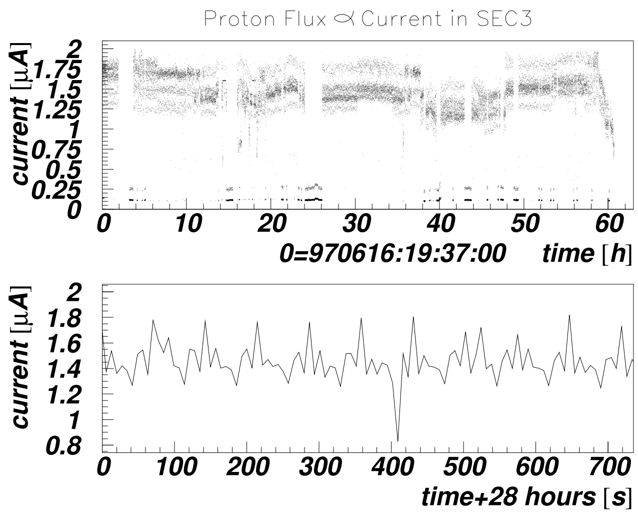

Figure 3: Current in the secondary emission chamber 3 (SEC3) during the first 60 hours. The current is proportional to the proton flux on the samples. The zoomed time intervall below shows a spill periode of about 7 seconds.

current is about 1.5 μA for a characteristic spill and dropps to a few nanoAmpere at spill breaks when no protons were delivered. A few spill breaks of 1/2 h to 1 hour are visible and the samples remained unirradiated in these periodes.

The absolute proton fluence was measured using an aluminum foil activation method. The amount of ^{24}Na generated in the Al-foil under proton irradiation is proportional to the fluence. ^{24}Na decays with a half life time of 15 hours and emits photons of 1.368 MeV which were measured in a γ-spectrometer immediately after an irradiation periode of 24 hours. We were using always a set of two foils, one foil with a size of 5×5 mm^2 the other with 10×10 mm^2. These sizes correspond to the area of either the dot sample or stip detector. The accumulated fluence as a function of time is shown in Fig. 4. During the first 60 hours the the PS delivered two spills per cycle and the fluence increased linearly up to 0.91×10^{15} p/cm^2 and 0.83×10^{15} p/cm^2 on the 5×5 mm^2 and 10×10 mm^2 samples. The proton flux on the 5×5 mm^2 samples is 9.8×10^{10} p/cm^2/spill which averages to 4.2×10^9 p/cm^2/s. The fluence measured with the small foils is systematically higher than the fluence on the bigger foils since protons sweep over samples and foils. The sweep area had a widths of approximately 1.5 cm and a height of 4 cm. Samples were adjusted to receive a maximum flux which was found to be in the lower center of the sweep area. Summation of the current from SEC3 [Fig. 3] is expected to be proportional to the fluence. If we normalize the current sum to reach the fluence given by the foil activation method we indeed recognize a linear dependence and agreement between the intermediate foil measurements and the current sum [Fig. 4]. The proton fluence was also measured by continously counting pulses delivered from the secondary emission chamber SEC1. The number of counts per spill is proportional to the induced charge in this chamber. Summation of pulses from SEC1 gives the fluence as a function of time which is shown in Fig. 4 as well. The graphs for SEC1 and SEC3 interpolate the data taken with the foil activation method and can be used to predict the fluence at each time between foil measurements. All three methods agree within an error of $\pm 2 \times 10^{13}$ p/cm^2. Fig. 5 shows the fluence on the samples for the whole irradiation

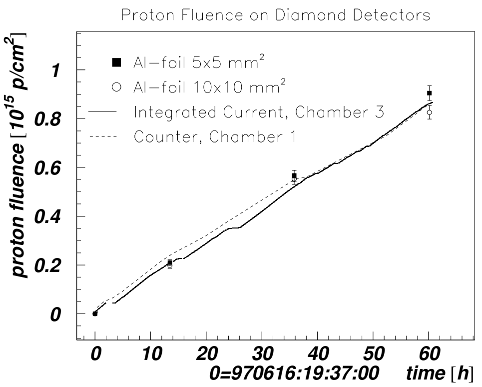

Figure 4: Proton fluence as a function of time up to 0.9×10^{15} p/cm^2. The fluence values obtained with the foil activation method and with both secondary emission chambers agree.

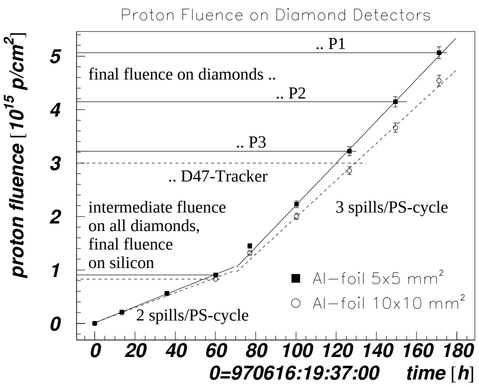

Figure 5: Proton fluence as a function of time up to 5×10^{15} p/cm^2. The slope of the fluence increases above 60 hours since the extraction changed from 2 to 3 spills per cycle. The graph shows the final fluences reached on each sample.

periode up to 5×10^{15} p/cm^2. After $\approx$60 hours the number of PS extractions was increased to three spills per cycle at a mean flux of 1.7×10^{11} p/cm^2/spill which corresponds to an average of 1.1×10^{10} p/cm^2/s. The final fluences which were reached on each sample are shown in Tab. 1. All samples were removed for an intermediate characterisation at a fluence of 0.9×10^{15} p/cm^2. The silicon diode was taken out of the irradiation at that level. The diamonds samples and the diamond strip tracker were reinserted and irradiated up to several 10^{15} p/cm^2. Sample CD12-P1 received the highest fluence of 5×10^{15} p/cm^2. The diamond strip detector DBDS-47 received a fluence of 3×10^{15} p/cm^2.

sample name	thickness [μm]	center electrode size [mm^2]	final fluence [10^{12} p/cm^2]
CD12-P1	716	7.1	5064 ± 111
CD12-P2	726	7.1	4146 ± 99
CD12-P3	709	7.1	3222 ± 84
DBDS-47	492	Tracker	3000 ± 30
Si-Diode	350	16.0	905 ± 30

Table 1: Final proton fluences on samples. The fluences were measured with a foil activation method.

2 Charge Collection Properties

The charge Q_{col} which can be collected at the electrodes after one charged particle traversed the diamond characterizes the performance of the detector. A minimum ionizing particle *mip* deposits 245 keV in $D = 500$ μm thick diamond. The energy which is necessary to excite one eh-pair in diamond is 13.6 eV. One obtains the number $\langle Q_{mip,\text{gen}} \rangle / D = 36$ e/μm of generated electrons or holes [3] Electron hole pairs seperate in the applied electric field and travel towards the electrodes where they induce a charge Q_{col}. The mean measured charge $\langle Q_{\text{col}} \rangle$ is related to the charge collection distance d of the diamond bulk and in an approximation one finds [3]

$$d \approx \frac{\langle Q_{\text{col}} \rangle}{\langle Q_{mip,\text{gen}} \rangle / D} = \frac{\langle Q_{\text{col}} \rangle}{36\ e/\mu\text{m}}, \tag{1}$$

which relates the charge collection distance to the collected charge at the electrodes.

2.1 Setup to Measure Charge Collection Distance

Fig. 6 shows a basic diamond readout and how charge collection distance was measured. A diamond sample is mounted underneath a colimated ^{90}Sr source. ^{90}Sr is a β-source and emits electrons with an endpoint energy of 2.28 MeV. A silicon diode below the diamond triggers on

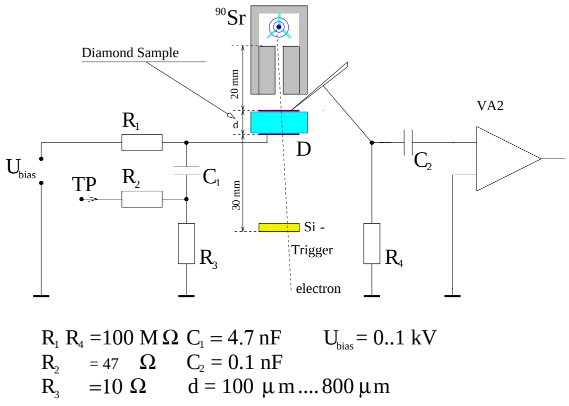

Figure 6: Setup for charge collection measurement in a diamond detector sample. The sample is illuminated by a colimated ^{90}Sr β source. A silicon diode below the diamond trigger the readout of the charge signal in diamond.

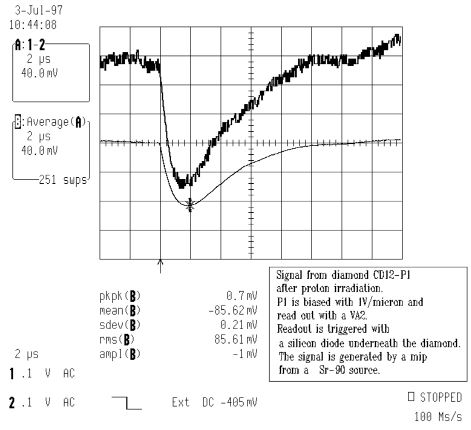

Figure 7: Signal of an event measured on diamond CD12-P1 after proton irradiation with 5×10^{15} p/cm^2. The signal is read out using one channel of a VA2 amplifier. The shaped signal has a peaking time of 2 μs. The waveform is averaged over several events.

electrons which traverse the diamond. The induced charge is measured with a charge sensitive amplifier which then gives the charge collection distance [Eq.1]. Calibration was done by measuring the charge signal either from a voltage pulse into a capacitor or by photo absorption from a γ-emitter in a silcion diode. Both methods give the same calibration constant with a calibration error of 5%. A characteristic signal from one irradiated diamond CD12-P1 measured at an applied electric field of 1 V/μm is shown in Fig. 7. The upper waveform, scope trace A, shows the shaped signal from the amplifier, the lower waveform is the average over several event samplings and shows an amplitude of 86 mV. Using a gain of 26.6 e/mV one obtains a mean collected charge of 2290 e which corresponds to a charge collection distance of 64 μm.

It is well known that the charge collection distance increases under illumination with γ or β radiation. On unirradiated samples an increase by a factor of 1.6 to 2.0 below 10 krad absorbed dose is observed. Above 10 krad charge collection distances stays constant. The increase at relatively low dose is called pumping. It is attributed to trap filling which then allows charge carriers to travel longer distances before being traped. A sample can be depumped by exposure to fluorescent light or heating (300 °C) and charge collection distance returns to its original value. Depumping is explained by releasing filled traps. The effect of pumping on irradiated samples will be described below.

2.2 Charge Collection at different Proton Fluences

Charge collection distance as a function of the applied electric field at different proton fluences is shown for all samples in Fig. 8. Normally we apply an electric field in a range from -1 V/μm to

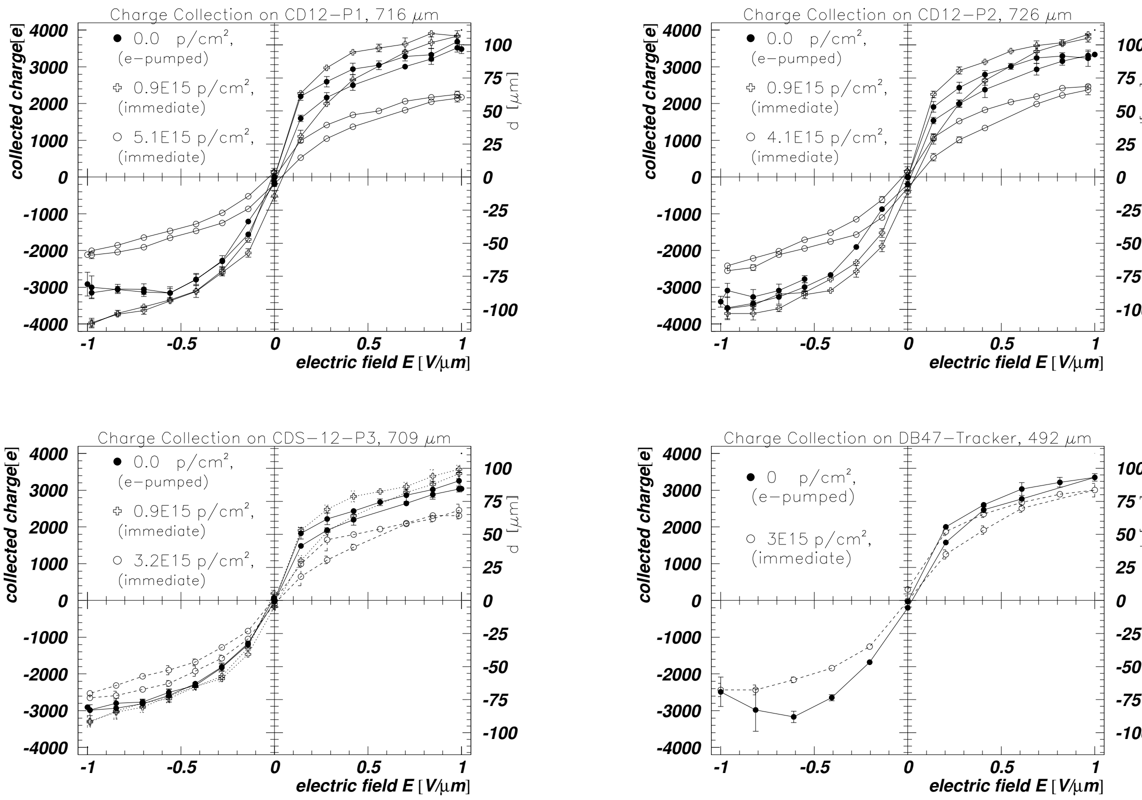

Figure 8: Charge collection distance as a function of the applied electric field at different proton fluences. Before irradiation samples were measured in their pumped state. The charge collection measurement after receiving a certain proton fluence was done immediately and without any exposure to light, which could have caused depumping.

$+1$ V/μm. In this range charge collection distance increases and saturates. Above $\approx \pm 0.8$ V/μm the velocity of charge carriers saturates and charge collection remains nearly constant. Looking at only charge collection at 1 V/μm and different proton fluences we observe no decreasing signal at 0.9×10^{15} p/cm^2 fluence. Instead charge collection even went up by a few percent compared to the measurement before irradiation.

The signal distribution at 1 V/μm is shown in Fig. 9. The charge distribution is described by a convolution of Landaus distribution function for thin detectors and a Gaussian and shown as a superimposed fitting curve. A small histogram taken at 0 V appears with a gaussian distribution at 0. Its standard deviation is about 350 e and represents the noise in the setup. Signal distributions at different fluences are superimposed. The most probable charge signal at the maximum of the fit curve remains constant up to the highest fluence of 5×10^{15} p/cm^2. The mean value at fluences above 3×10^{15} p/cm^2 decreases due to less events with high charge signal. Since the charge collection distance is related to the mean charge signal [Eq. 1] we observe a decreasing charge collection distance above 3×10^{15} p/cm^2.

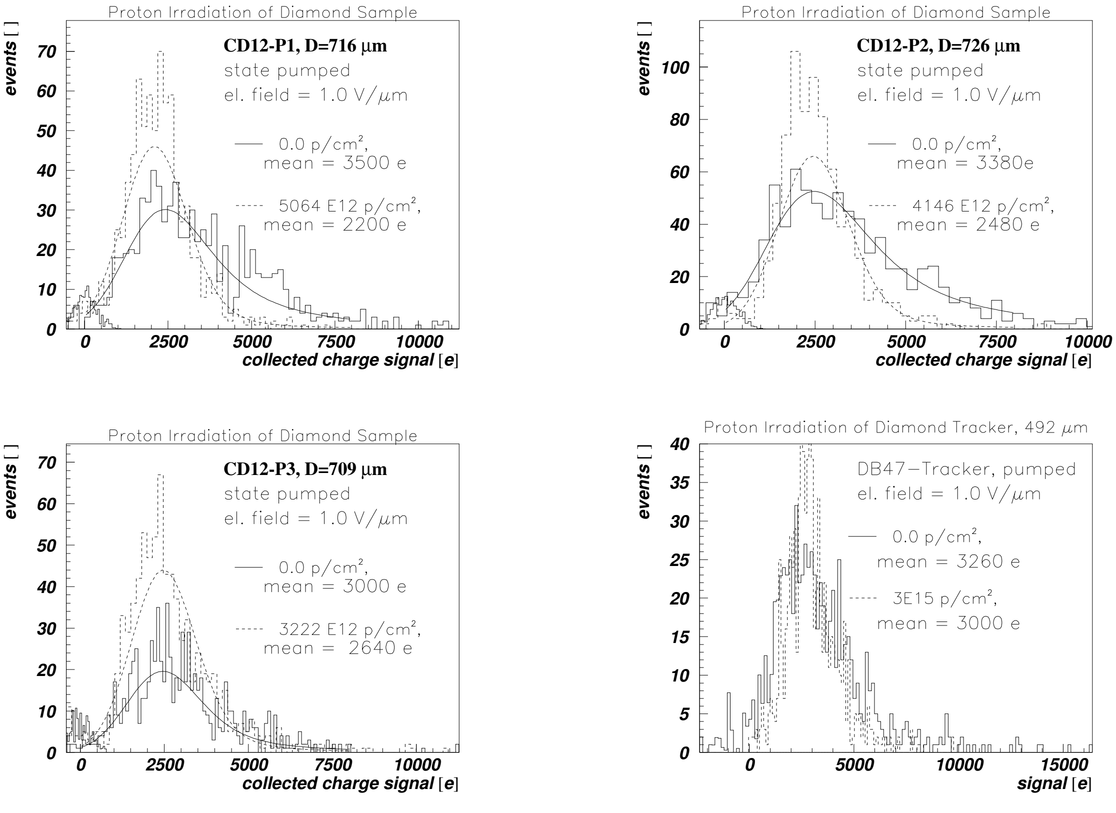

Figure 9: Charge signal distribution at a bias voltage of 1 V/μm on irradiated diamond samples at different fluences immediately after proton irradiation.

Fig. 10 shows the charge collection distance as a function of the proton fluence. These measurements were done immediately after irradiation and the samples only had a rest for about two hours in darkness in order to cool down before they were measured. The charge collection distance decreases above 2×10^{15} p/cm^2. The charge collection distance normalized to the pumped value before proton irradiation gives a linear decrease down to 60 % at 5×10^{15} p/cm^2.

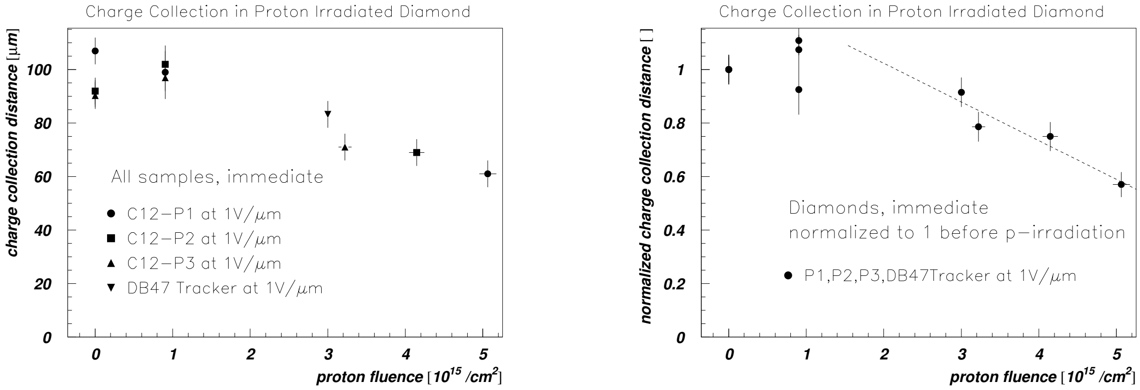

Figure 10: Charge collection distance in CVD diamond measured immediately after irradiation at different proton fluences. On the right graph the charge collection distance is normalized to its pumped value before irradiation.

2.3 Pumping with Electrons after Proton Irradiation

All samples were depumped after irradiation by exposure to fluorescent light for several hours. Exposure to fluorescent light empties traps and charge collection distance decreases [4]. Fig. 11 shows the charge collection distance as a function of time at constant voltage under exposure to the relatively low dose of electrons from ^{90}Sr. In the first measurement at time 0 charge collection is relatively low. It increases during measurements and saturates above 10 hours exposure in the characterization station which can be seen by looking at the normalized charge collection distance. The fully pumped (saturated) charge collection distance is the same as the value immediately after

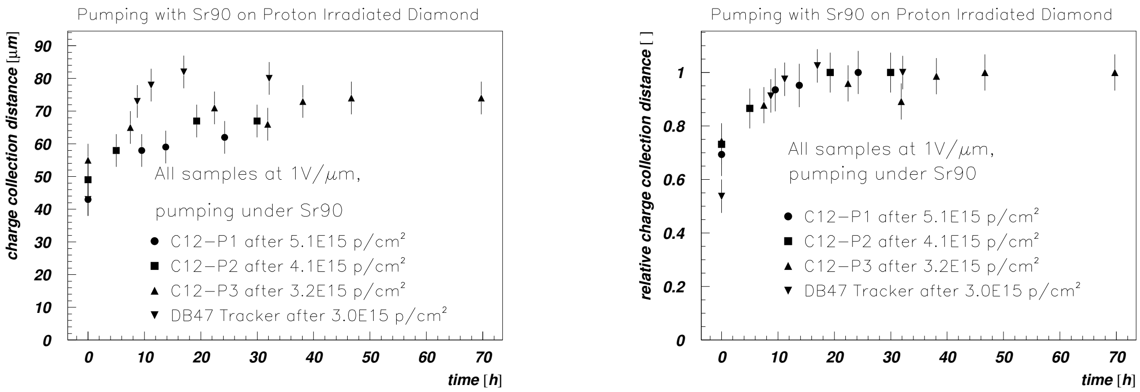

Figure 11: Charge collection distance in irradiated CVD diamond measured during pumping with ^{90}Sr at different p-fluences. On the right graph the charge collection distance is normalized to its pumped saturation value.

proton irradiation which means that the diamond pumped during irradiation. It is likely that pumping during proton irradiation occured within the first minutes in the beam since the proton flux was much higher than what could be radiated by our 37 MBq ^{90}Sr source in the lab.

The pumped charge collection at different proton fluences is shown in Fig. 12. Comparison with Fig. 10 confirms that the charge collection distance can be reproduced by exposure to a relatively low dose of ^{90}Sr. The pumped values can be normalized to the pumped value before irradiation which is shown in the right figure 10. A linear fit to the values above 3×10^{15} p/cm^2 intersects the graph of values from before 1×10^{15} p/cm^2 at a fluence of 2×10^{15} p/cm^2. Thus we observe no decrease in charge collection distance before 2×10^{15} p/cm^2 and conclude these samples to be

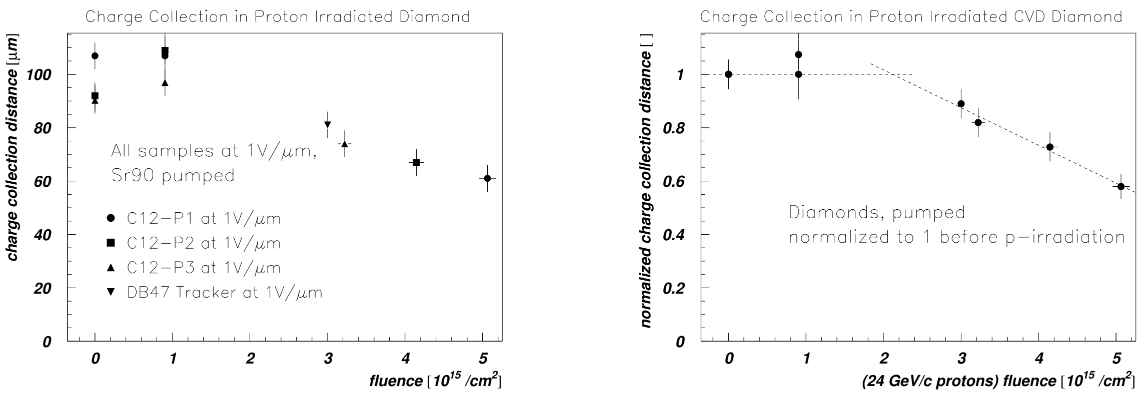

Figure 12: Charge collection distance in CVD diamond in dependence of the p-fluence. Samples were depumped under fluorescent light after proton irradiation and then pumped under ^{90}Sr. Only fully pumped charge collection values are shown. On the right graph the charge collection distance is normalized to its pumped value before irradiation.

radiation resistant up to 2×10^{15} p/cm^2. Above 2×10^{15} p/cm^2 we observe a linearly decreasing charge collection distance with a slope of $-14\%/10^{15}$ p/cm^2. At 5×10^{15} p/cm^2 charge collection distance is decreased by 40%.

Charge collection values are listed in Tab. 2 at different proton fluences and compare the measurement immediately after irradiation with the pumped value after a depumping and pumping cycle. It shows the decrease in charge collection distance mentioned above and confirms that charge collection measurements are reproducible after depumping and pumping on all samples and that samples were in a pumped state during proton irradiation.

sample name	fluence [10^{12} p/cm^2]	state	$\langle Q_{\mathrm{col}} \rangle$ at 1 V/μm [e]	d [μm]
CD12-P1	0	pumped	3852	107
	905	immediate	3560	99
	5064	immediate	2196	61
		pumped	2232	62
CD12-P2	0	pumped	3312	92
	905	immediate	3672	102
	4146	immediate	2480	69
		pumped	2412	67
CD12-P3	0	pumped	3240	90
	905	immediate	3492	97
	3222	immediate	2556	71
		pumped	2660	74
DB47-Tracker	0	pumped	3276	91
	3000	immediate	2988	83
		pumped	2920	81
Silicon-Diode	0		30500	
	905	immediate	no signal	

Table 2: Collected charge Q_{col} and charge collection distance d of diamond samples and silicon diode at different proton fluences.

3 Particle Induced Currents during Proton Irradiation

Protons induce a current $I_{\rm pic}$ in diamond which adds to the dark current and which is given by the mean number of collected charges $\Delta Q_{\rm col}$ in a time intervall Δt.

$$I_{\rm pic} = \frac{\Delta Q_{\rm col}}{\Delta t}. \tag{2}$$

A number ΔN_p of protons interact in diamond and generate electron-hole pairs where the ensemble of either carrier types has a charge $\Delta Q_{p,\rm gen}$ of opposite sign. Using the charge collection distance d [Eq.1] one obtains

$$I_{\rm pic} = d \cdot \frac{A}{D} f_p \frac{\Delta Q_{p,\rm gen}}{\Delta N_p}, \tag{3}$$

with the proton flux f_p, sample thickness D and contact area A. This equation relates the charge collection distance to the particle induced current.

3.1 Setup to Measure Current during Irradiation

All diamond samples were biased with 100 V applied between both electrodes. Biasing of samples is a realistic operation condition and allows to measure induced currents during irradiation. The temperature during irradiation was stable close above roomtemperature for either diamond and silicon. Fig. 13 shows the schematics for voltage biasing and current measurement on one sample. Box 1 contains the biasing voltage with a pA-current meter. Box 2 with the diamond sample inside was located 25 m away inside the irradiation zone and connected with two BNC lines to the biasing in box 1. The Silicon diode was biased with 74 V. Bias resistors were 10 kΩ and would not introduce significant voltage drops below $\approx 100\ \mu$A.

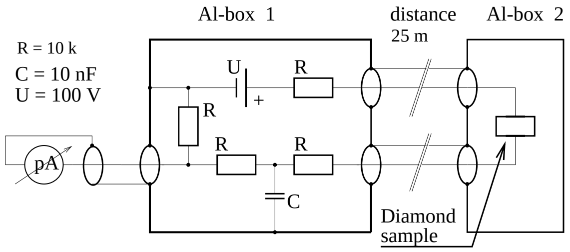

Figure 13: Circuitry for biasing diamond and silicon samples and measuring currents during irradiation.

3.2 Current during Irradiation

The particle induced current on diamond sample P1 is shown in Fig. 14. The left measurement shows the current which was recorded in 300 ms on-spill periodes whereas the measurement to the right shows the current during off-spill periodes. The on-spill current is in order of 10 μA and follows the proton flux. It shows that the current during spill breaks vanishes immediately and is in the order of nanoAmpere as it is during off-spill periodes (right figure). This means that the current measured in diamond is a real particle induced current and has no offset due to leakage current as e.g. known in silicon. The particle induced current is with 10 μA at least 10^4 times higher than the off-spill current. The off-spill current is dominated by noise. It is known to be several picoAmpere.

The on-spill current shows strong variations which could be actually true flux variation as it was seen in the measurement on the secondary emission chamber SEC3 3. The measurements on sample P2, P3 and DB47 show a similar behavior [Fig. 15, 16,17]. Their induced currents correlate in a first view. At a closer look one observes differences and spill breaks in one sample which do not appear in the other. This is possible since the on-spill current could be only measured on one sample per spill. The short time intervall of 300 ms made it impossible to switch to a second or more samples in the same spill. The on-spill current on P3 could not be measured since the cable lost contact after installation in the irradiation zone. Fig. 18 compares dirctly the proton

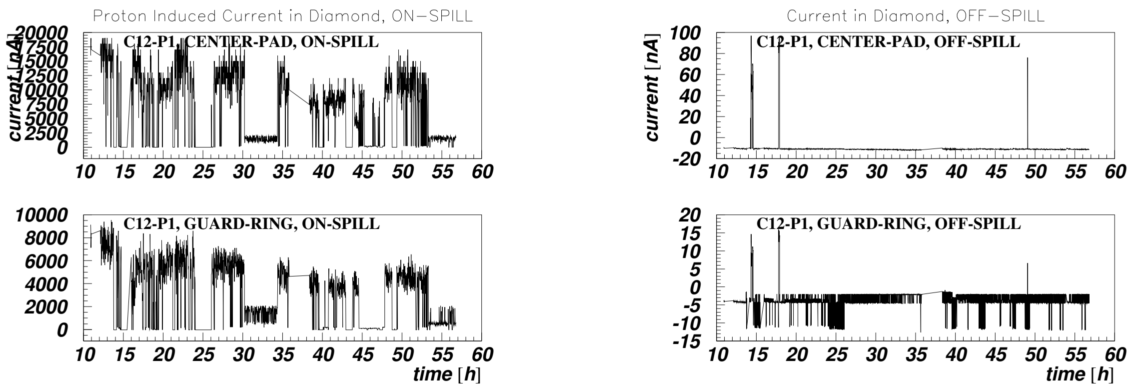

Figure 14: Current in diamond P1 during during p-irradiation.

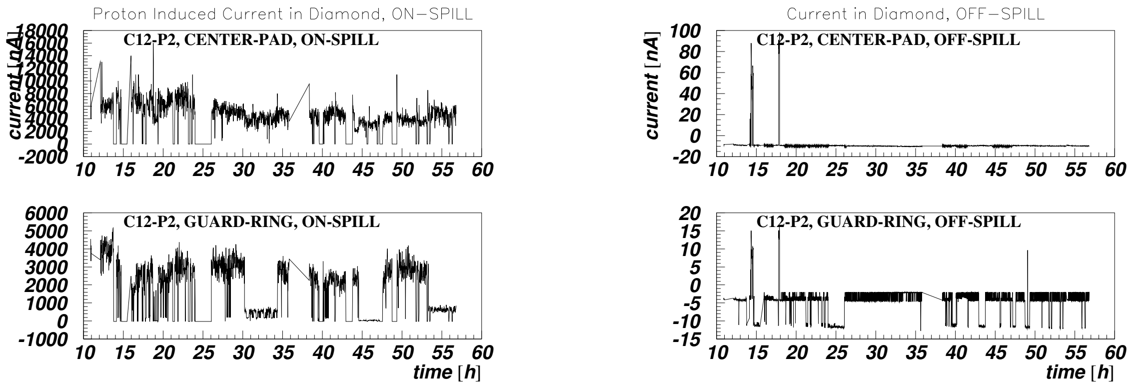

Figure 15: Current in diamond P2 during during p-irradiation.

flux measured in chamber SEC3 with the on-spill current in diamond (DB47). The graph of the proton flux includes all spills whereas the on-spill current in the diamond was taken only every 10 spills. The current in the diamond vanishes between 35 h and 35 h although protons pass the chamber. This happens since stearing magnets changed temporarily to a different timing and moved the beam by several milimeter. The same effect was measured in the silicon diode [Fig. 19]. The off-spill current in silicon is higher than the on-spill current in diamond and increases as soon as the irradiation starts. The on-spill current increases due to the increasing leakage current. The off-spill current anneals during spill breaks.

3.3 Charge Collection Distance and Induced Current

It is interesting to verify the relation between the charge collection distance and the particle induced current [Eq. 3]. Using the measured values for charge collection distance of $d \approx 80$ μm, a characteristic induced current of 8 μA, an electrode area of 7 mm^2, a sample thickness of $D \approx$ 700 μm and the proton flux of $\approx 10 \times 10^{10}$ p/cm^2/spill at a spill length 300 ms/spill one calculates the number of generated charges $\Delta Q_{p,\mathrm{gen}}$ per incident protons ΔN_p

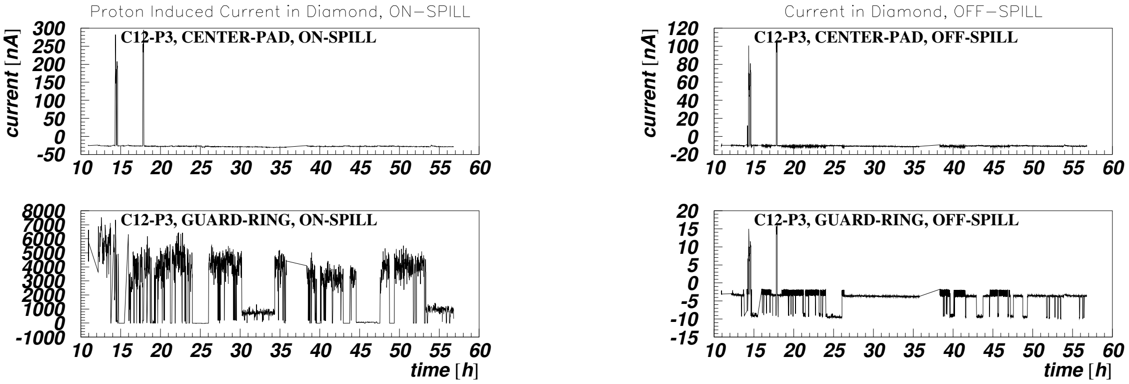

Figure 16: Current in diamond P3 during during p-irradiation. The contact to the center pad of P3 was lost since the start of the irradiation.

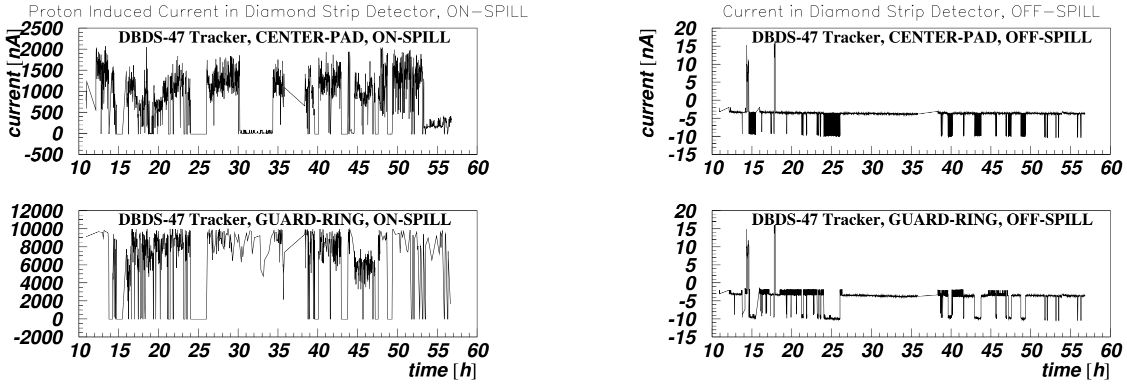

Figure 17: Current in the diamond strip detector DBDS-47 during during p-irradiation.

$$\frac{\Delta Q_{p,\mathrm{gen}}}{\Delta N_p} = \frac{8\ \mu\mathrm{C/s}\cdot 6.25\cdot 10^{18} e/\mathrm{C}}{80\ \mu\mathrm{m}}\cdot\frac{700\ \mu\mathrm{m}}{7\cdot 10^6\ \mu\mathrm{m}^2}\cdot\frac{0.3\ \mathrm{s/spill}}{10\cdot 10^{10}\cdot 10^{-8}\ p/\mu\mathrm{m}^2/\mathrm{spill}} \quad (4)$$

$$= 6.25\cdot 0.3\times 10^4\ \mathrm{e/p} \quad (5)$$

$$\approx 20000 \text{ generated charge carriers} \quad (6)$$

The number of generated charge can be estimated using the differential energy loss of 1.75 MeVcm^2/g in carbon for protons with a momentum of 24 GeV/c [5] and the density 3.5 g/cm^2 of diamond. In a 700 μm thick diamond we obtain a mean energy deposit of 429 keV. Since 13.6 eV are necessary to generate one eh-pair one finds the number $\approx$ 30000 generated charge carriers which agrees roughly with the measured value.

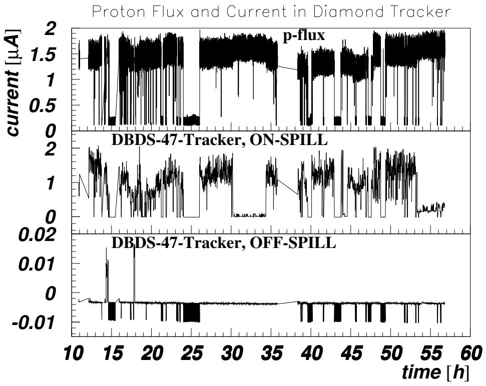

Figure 18: Current in the diamond strip detector DBDS-47, center pad, during p-irradiation. The current was measured on- and off-spill.

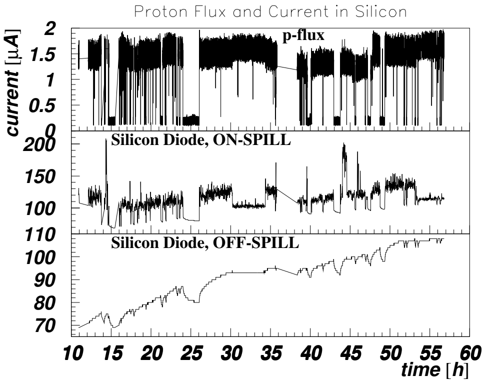

Figure 19: Current in a silicon diode, during p-irradiation. The current was measured on- and off-spill.

4 Conclusion

CVD diamond detector samples were irradiated with 24 GeV/c protons up to a fluence of 5×10^{15} p/cm^2. The most probable charge signal of the detectors remains unchanged up to the highest fluences. The mean charge signal which is proportional to the charge collection distance remains unchanged up to 2×10^{15} p/cm^2. Above 2×10^{15} p/cm^2 we observe a linear decrease in charge collection distance with a slope of -14 %/10^{15} p/cm^2.
The dark current before and after irradiation is unchanged. The current during irradiation shows a prompt response to presence of the spill and correlates with the proton flux. The off-spill current (absence of protons) is below the accuracy of the measurement. The on-spill current is of several microAmpere and its response to protons does not change up to a fluence of 10^{15} p/cm^2 (no currents were recorded above this fluence). The particle induced current is expected to be proportional to the charge collection distance. Using the measured charge collection one can calculate the induced current which agrees with the measured induced current.

A silicon diode participated in the same irradiation up to 0.9×10^{15} p/cm^2. Its off-spill current is higher than the on-spill current in diamond. The leakage current starts increasing immediately after exposure to the first spill. The on-spill current increases due to the increasing leakage current. The silicon diode anneals during spill breaks and leakage current decreases slowly. After 0.9×10^{15} p/cm^2 the charge signal was unmeasurable because of high noise due to too high leakage current.

We conclude that CVD diamond detectors perform well in terms of charge collection and current up to 2×10^{15} p/cm^2 and show no sign of detoriation. Above 2×10^{15} p/cm^2 we observe a linearly decreasing charge collection down to 60% at 5×10^{15} p/cm^2.

5 Acknowledgements

We would like to acknowledge the help of M. Glaser, F. Lemeilleur and A.Taffard during irradiation and dosimetry.

References

[1] S. Han *et al.* (RD42 Collaboration). "Proton Irradiation Studies of CVD Diamond Detectors", (1996). internal report.

[2] DeBeers Industrial Diamond Division Ltd., Charters, Sunninghill, Ascot, Berkshire, SL5 9PX England.

[3] S. Zhao. *"Characterization of the Electrical Properties of Polycrystalline Diamond Films"*. PhD thesis, Ph.D. Dissertation, Ohio State University, (1994).

[4] D. Meier *et al.* (RD42-Collaboration). "Diamond as a Particle Detector". In *EuroDiamond 96*. It. Phys. Soc., Conf. Proc., **52** (1996) 105.

[5] Particle Data Group. "Review of Particle Properties". *Phys. Rev.*, **50(3), (1994).**